International Journal of Nanomedicine

Dovepress
Taylor & Francis Group

Open Access Full Text Article

ORIGINAL RESEARCH

Formulation and Application of a Human Insulin-Like Growth Factor 1-Loaded Transfersomal System to Enhance Skin Wound Healing in Diabetic Rat Models

Fahimeh Nojoki[1], Kianoush Dormiani[2], Mahboobeh Forouzanfar[2], Amin Derakhshan[2], Mohammad Hossein Nasr-Esfahani[2], Sanaz Sedghi Esfahani[3], Parto Nasri[4]

[1]Research Center for New Technologies in Life Science Engineering, University of Tehran, Tehran, Iran; [2]Department of Animal Biotechnology, Cell Science Research Center, Royan Institute for Biotechnology, ACECR, Isfahan, Iran; [3]Department of Biology, Faculty of Science and Technology, ACECR Institute of Higher Education (Isfahan Branch), Isfahan, Iran; [4]Department of Pathology, Isfahan University of Medical Sciences, Isfahan, Iran

Correspondence: Kianoush Dormiani, Department of Animal Biotechnology, Cell Science Research Center, Royan Institute for Biotechnology, ACECR, Salman Street, Royan Street, PO Box: 816513-1378, Isfahan, Iran, Tel +98 31 95015691, Fax +98 31 95015687, Email k_dormiani@royaninstitute.org

Background: Transdermal drug delivery is a local and non-invasive method for treating skin diseases that offers advantages such as sustained and long-term drug release.

Methods: In this study, transfersomes (TFs) containing human Insulin-like growth factor 1 (TF/hIGF-1) were prepared and characterized as an effective transdermal drug delivery system to improve skin wound healing in diabetic models. TFs were prepared using the film hydration method and characterized by various methods.

Results: Pre-release evaluation confirmed the controlled release of human insulin-like growth factor (hIGF-1) supported by TEM images, showing dispersed spherical shapes with particle sizes below 100 nm. In vitro studies of these nanovesicles demonstrated that encapsulation significantly improved the stability and functionality of hIGF-1, enhancing cell migration and complete closure of cell monolayer gaps. In vivo studies on diabetic rats treated with TF/hIGF-1 hydrogel revealed accelerated wound healing compared to controls. Histopathological analysis also showed increased epidermal thickness and dermal protrusions, indicating enhanced healing effects.

Conclusion: Overall, this study demonstrated that hIGF-1 released from TF/hIGF-1 in a controlled manner could effectively promote re-epithelialization and granulation tissue formation in diabetic wounds of animal models compared to controls. These findings suggest a promising and effective approach for potential use in treating diabetic wounds.

Keywords: insulin-like growth factor 1, dermal drug delivery, diabetic wound, nanoparticles, transfersome

Introduction

Recent clinical studies have demonstrated the significant therapeutic effects of growth factors such as epidermal growth factor, vascular endothelial growth factor, and insulin-like growth factors in regenerative medicine applications.[1] These protein factors when used as recombinant drugs, stimulate cell proliferation, migration, and differentiation to facilitate damaged tissues repair. However, after in vivo administration, they are enzymatically degraded at their site of action, resulting in a relatively short half-life (less than 15 min). The hIGF-1, also known as somatomedin-C, is a peptide composed of 70 amino acids in a single strand with three disulfide bridges and a molecular mass of 7.6 kDa.[2,3] Recombinant hIGF-1 (Mecasermin) has been approved by the US Food and Drug Administration (FDA) for the treatment of severe primary IGF-1 deficiency or growth hormone (GH) gene deletion with neutralizing antibodies to GH in children.[4,5] Beyond endocrine therapy, hIGF-1 contributes to the regulation of glucose metabolism and bone

https://doi.org/10.2147/IJN.S564241
Received: 17 September 2025
Accepted: 10 January 2026
Published: 19 February 2026

formation, and has therefore been investigated for its therapeutic potential in diabetes mellitus and osteoporosis.[6,7] Moreover, hIGF-1 acts as a key regenerative growth factor, stimulating stem-cell proliferation, migration, and differentiation into fibroblast-like cells and other reparative phenotypes that support wound healing and tissue regeneration.[8,9] This factor also acts as a mitogen for keratinocytes, stimulating keratinocyte proliferation and migration,[10,11] and indirectly increases angiogenesis by stimulating Vascular Endothelial Growth Factor (VEGF).[12] Consequently, hIGF-1 is considered an important factor in the wound healing process due to its stimulatory impact on epidermal stem cell proliferation and differentiation, as well as re-epithelialization and vascularization in the wound bed. On the other hand, as reported in the literature, impaired healing of diabetic wounds is due to ineffective angiogenesis resulting from glucose-dependent changes in capillary permeability and defects in endothelial and endothelial progenitor cells.[13,14] The expression levels of many growth factors, such as hIGF-1, are reduced in the basal keratinocyte layer and fibroblasts, leading to delayed wound healing.[15,16] It has also been shown that hIGF-1 levels are reduced in streptozotocin-induced diabetic wounds in rats.[17] Additionally, the reduced levels of hIGF-1 have been identified as the directly responsible for endothelial dysfunction in diabetic individuals.[18] Numerous studies have demonstrated that the application of growth factors can significantly enhance the healing of wounds of this nature.[19] For example, hIGF-1, produced by mesenchymal cells like dermal fibroblasts and dermal papillae,[20] plays a critical role in the proliferation, survival, and maintenance of skin cells and tissue balance.[21,22] It is also effective in treating various wounds by stimulating collagen synthesis and acting as a potent mitogen for keratinocytes and fibroblasts.[10,23,24] Similarly, overexpression of hIGF-1 in diabetic wounds through cell-based non-viral gene therapy has exhibited a significant improvements in diabetic wound healing.[25]

Currently, hIGF-1 is manufactured using recombinant DNA technology and has been suggested as a therapeutic protein for various skin conditions, including wound healing.[26,27] While the oral route is appealing for drug delivery due to its non-invasive nature and ease of administration, it is unsuitable for peptide drug administration because of challenges like rapid pH-induced or enzymatic degradation and poor absorption.[28] Intravenous injection of hIGF-1 can lead to adverse effects such as hypoglycemia, changes in mental status, and in severe cases, death.[23,29] In contrast, dermal drug delivery is a local and non-invasive method that offers advantages such as sustained drug release and cost-effectiveness. Delivery of growth factors like recombinant hIGF-1 through the dermal route can enhance collagen synthesis by skin cells and expedite wound healing.[16] Despite these advantages, the use of this type of drug delivery is limited to molecules with small sizes (less than 500 daltons) and lipophilic properties to pass through the stratum corneum, a dermal barrier against external agents.[30] Nanocarrier-based drug delivery systems are utilized to transport larger drug molecules into the skin. Therefore, the use of lipid nanoparticles and dressing gels has shown promise for efficient dermal delivery of therapeutic proteins such as hIGF-1. Various dressings have been designed to incorporate active pharmaceutical ingredients for wound healing applications. For instance, the electrospun Janus wound dressing, which can include multiple chambers for loading pharmaceutical ingredients into different polymer matrices, has demonstrated its versatility in wound healing.[31] Multifunctional electrospun fibrous coatings (EFCs) have also been developed with an inner three-layer core-sheath nanostructure to individually load pharmaceutical ingredients in the shell, middle, and core sections. Hydrogels, another type of polymer matrix, have the ability to retain significant amounts of water and drugs, releasing them gradually.[32] Hydrogels can also regulate drug release by altering the gel structure in response to environmental stimuli, such as pH, temperature, and ionic strength.[33]

Using nanoparticles not only improves the permeability and effectiveness of therapeutic agents but also can reduce the required dose of administration, resulting in a substantial reduction of side effects and less frequent medication dosing, which is more cost-effective.[23,34] TF, as a type of lipid nanoparticle, can slowly release its cargo into the target organs without causing outstanding toxicity. It is indicated that TF functions as an ultra-deformable nanoparticle, which can traverse the epithelium with extensive elasticity due to the presence of phospholipids together with an edge activator (EA).[35,36] The EAs, including tweens, spans, and sodium salt of deoxycholate, are ionic surfactants that weaken the lipid bilayers of the vesicles.[37]

The aim of this study is to develop a TF nanoparticle containing hIGF-1 (TF/hIGF-1) for sustained release of the active ingredient in diabetic wounds through transdermal administration. The platform is designed to release hIGF-1 continuously, prolonging the presence of the growth factor at the wound site, and effectively promoting diabetic wound healing. To synthesize the nanoparticle, phosphatidylcholine (Phospholipon 90 H) and sodium deoxycholate (SDC) were

utilized as oil phases and surfactants, respectively, with hIGF-1 added to the aqueous phase. After constructing the nanoparticle using the film hydration method, it was characterized based on optimal values of particle size, polydispersity index, zeta potential, and encapsulation efficiency. In vitro studies were conducted to validate the encapsulation efficiency, improved stability, sustained release, functionality of hIGF-1, and enhanced cell migration. Subsequently, the in vivo application of TF/hIGF-1 nanoparticle on animal models with diabetic wounds demonstrated faster and more complete wound healing compared to control groups.

Materials and Methods

Materials

Phospholipon 90 H, a hydrogenated soy phosphatidylcholine, was purchased from Lipoid GmbH (Germany). Carboxymethylcellulose (CMC) was obtained from Sigma-Aldrich (USA). Recombinant human IGF-1 was purchased from Peprotech (USA). Streptozotocin (STZ), hematoxylin and eosin (H&E) stain, phosphate-buffered saline (PBS) buffer, ketamine hydrochloride, xylazine, sodium deoxycholate (SDC), paraformaldehyde, hydrochloric acid (HA), dimethyl sulfoxide (DMSO), ethanol, and methanol were obtained from Sigma-Aldrich (USA), while other solvents were purchased from Merck Company (Germany).

Preparation of TF

The different TF vesicles were prepared using the film hydration method.[38] A specific amount of Phospholipon 90 H and SDC as an edge activator (4:1 w/w ratios) were dissolved in 2 mL of chloroform in a 50 mL round-bottom flask. The solvent was evaporated using a rotary flash evaporator (Heidolph, Germany) at 50°C and 150 rpm under vacuum to produce a dry lipid film. The thin film was then hydrated with a 50 μg/mL hIGF-1 solution in PBS buffer (0.1 M, pH 4) at a w/w ratio of 200:1 by rotating for 2 h at 37°C and 70 rpm without vacuum. The multilamellar vesicles (MLVs) and small unilamellar vesicles (SUVs) were reduced in size through sonication. Once the TF/hIGF-1 vesicles were formed, they were extruded and filtered to isolate vesicles of the desired size. The unloaded TFs were also prepared and characterized using the same method.

Physicochemical Characterization of TF/hIGF-1

The hydrodynamic size, zeta potential, and polydispersity index (PDI) of the prepared TF/hIGF-1 were determined using dynamic light scattering (DLS) with a Malvern Instruments system (UK). Encapsulation efficiency (EE) and drug loading (DL) were calculated using the equations provided below (n = 3). The concentration of hIGF-1 was also measured using the Bradford protein assay.[39]

$$\mathrm{EE}(\%) = \frac{\text{Weight of hIGF1 in NPs}}{\text{Total weight of hIGFI used in formulation}} \times 100$$

$$\mathrm{DL}(\%) = \frac{\text{Weight of hIGF1 in the NPs}}{\text{Total weight of the NPs}} \times 100$$

Evaluation of TF/hIGF-1 Morphology

The morphology of the nanoparticles was evaluated using transmission electron microscopy (TEM). For this, a drop of TF suspension was applied to a carbon-coated grid. After 30 seconds, excess liquid was removed with filter paper, and a 1% (w/v) uranyl acetate solution was used as a negative stain. The morphology of TF/hIGF-1 was examined using transmission electron microscopy at 100 kV.

Stability Analysis of Released hIGF-1

To assess the short-term stability of the encapsulated hIGF-1 post-release from the TF/hIGF-1 nanoparticles, SDS-PAGE analysis was performed. Dialysis method was employed with samples collected at various time intervals ranging from 2 to 48 hours. Dialysis was carried out using membranes with a molecular weight cut-off of 10 kDa. These membranes

were immersed in a pH 7.4 PBS buffer and incubated at 37°C with a rotation speed of 70 rpm. The TCA precipitation and acetone wash procedure were utilized to concentrate the low-concentration protein samples collected from the PBS dialysis buffer. At each time point, 1 mL of PBS was withdrawn, and 200 µL of 100% trichloroacetic acid was added to the protein solution. Following a brief vortex, the samples were chilled on ice and then centrifuged at 4°C and 14,000 rpm for 5 minutes. The supernatants were discarded, and the precipitates were washed twice with 100% acetone. After acetone evaporation, the samples were heated at 95°C for 10 minutes. The dried samples were then loaded onto a 15% SDS-PAGE gel and subjected to electrophoresis. Subsequently, the bands were visualized using silver staining.[40]

Evaluation of hIGF-1 In vitro Release Kinetics

The release profile of hIGF-1 in TF/hIGF-1 was analyzed using the dialysis method. For this, equal amounts of free hIGF-1, TF/hIGF-1, and unloaded TF were placed in dialysis membranes with a molecular weight cut-off of 10 kDa separately and dialysis was carried out according to the previous section. Sampling was carried out at different time points over a period of 1 to 48 h to monitor the release of hIGF-1. The amount of released protein was quantified using the Bradford method, and a release profile was constructed. The kinetic profile model of hIGF-1 release from the nanoparticles was also analyzed and fitted using various release models.

Synthesis of CMC Hydrogel

CMC is a water-soluble polymer widely used in various fields, including as a drug carrier for therapeutic applications.[41] The preparation of a CMC hydrogel containing TF, hIGF-1, and TF/hIGF-1 was carried out following the method by Che Nan et al.[42] Briefly, the hydrogels were prepared by slowly immersing the sodium salt of CMC in water at 70°C, resulting in a final concentration of 20% w/v CMC in water. The mixture was then stirred for 4 h at 70°C to completely dissolve the salt and form a transparent, uniform wet gel.

In vitro Pharmacokinetic Study of TF/hIGF-1

Cell Culture

NIH-3T3 cells were obtained from the National Cell Bank of Iran (Pasteur Institute of Iran, Tehran). The cells were cultured in Dulbecco's Modified Eagle Medium (DMEM) supplemented with 10% fetal bovine serum (FBS), 1% Glutamax, and 100 U/mL ampicillin and streptomycin (all from Gibco, USA) at 37 °C and 5% CO_2. The culture medium was replaced every two days, and when the confluence reached approximately 80%, the adherent cells were trypsinized using 0.05% Trypsin-EDTA (Gibco, USA) and subcultured. Cryopreservation and recovery of the cells were performed according to standard procedures.

MTS Assay

The viability of NIH-3T3 fibroblast cells was assessed after treatment with TF/hIGF-1. For this, NIH-3T3 cells were initially seeded in 96-well plates at a density of 4000 cells per well in complete culture medium. After 24 h of incubation, the medium was replaced with DMEM containing 0% serum and the plates were further incubated for 6 h. Subsequently, samples including a negative control, free hIGF-1 in a dilution series ranging from 200 to 6.25 ng/mL, empty TF, and TF/hIGF-1 were added to the wells. The cells were then cultured under the same conditions for 24, 48 and 72 h with experiments conducted in triplicate. Following each incubation period, 100 µL of MTS reagent (Abcam, USA) was added to the wells and incubated for 4 h. The absorbance was measured at 450 nm with 650 nm as the reference wavelength. The absorbance values were directly correlated with the number of viable cells in the culture.

In vitro Wound Healing and Cell Migration Assay

After determining the optimal dose of TF/hIGF-1 and hIGF-1 on the NIH-3T3 cell line, a cell migration and wound healing assay was performed using wound inserts in a 12-well plate. Briefly, when the cell culture reached a density above 90%, the culture medium was replaced with serum-free DMEM, and wound inserts were placed in each well, creating a 500 µm wide cell gap to measure cell migration and wound healing rates. Subsequently, different drug doses

were added to each group, and images of wound closure were captured at various time points (0, 24, 48, 96, 144 h) using a light microscope. The cell migration rate was then analyzed using Image J software (version 1.52).

In vivo Application of TF/hIGF-1 in Wound Healing Study

Induction of Diabetic Animal Model

The chronic STZ-diabetic rat is a valuable model for creating a diabetic rat to test therapeutic approaches for alleviating chronic diabetic complications in humans. Intraperitoneal and intravenous injections of STZ are common methods for inducing stable hyperglycemia.[43] In this study, adult male Wistar rats aged 3 months (weighing 200 ± 50 g, obtained from the Laboratory Animal Center at Royan Institute) were used to establish the diabetic model. For this purpose, the rats were fasted overnight before drug administration but had free access to water. The next day, STZ dissolved in normal saline with a final concentration of 45 mg/mL was intraperitoneally injected at a dose of 60 mg/kg of body weight. After two days of injection, blood glucose levels were measured using a Glucometer (ACCU-CHEK, Switzerland) by sampling the tail vein of the rats, and those with blood glucose levels reaching 250 mg/dl were considered diabetic. This study was conducted on male Wistar rats after obtaining approval from the Ethics Committee for Experimental Animals at the Royan Institute (ethics code: IR.ACECR.ROYAN.REC.1400.041) and in accordance with the Guidelines for the Care and Use of Laboratory Animals in Iran.[44]

Animal Grouping and Treatment

In this study, two main groups of rats were used, normal and diabetic. Three similar wounds were created on the back of each rat in both groups with one serving as a control. The normal and diabetic animals were randomly divided into 6 groups, each consisting of 4 rats, as outlined below:

1. Non-diabetic group + hIGF-1 hydrogel
2. Non-diabetic group + TF hydrogel
3. Non-diabetic group + TF/hIGF-1 hydrogel
4. Diabetic group + hIGF-1 hydrogel
5. Diabetic group + TF hydrogel
6. Diabetic group + TF/hIGF-1 hydrogel

Two types of control wound dressings were applied in each group:

1. Groups without any dressing
2. Groups with dressing containing hydrogel only

The rats were housed in an air-controlled environment with 55% humidity, a 12-h dark/light cycle, and a temperature of 25°C, with free access to food and water. The rats were carefully monitored and maintained following standard protocols. Treatments were administered every other day for each group until the first wound closed. The amount of hydrogel applied per wound was 100 μL of gel/cm^2 containing 250 ng/mL of hIGF-1.

Histological Analysis

After the initial wound had healed, histological evaluation was performed using established techniques.[45,46] Adult male rats were euthanized in accordance with the guidelines of the American Veterinary Medical Association (AVMA).[47] The rats were placed in a chamber of appropriate size that was not pre-filled with CO_2. The gas from a compressed cylinder was gradually introduced at a controlled flow rate, displacing 30% to 70% of the chamber volume per minute to ensure a smooth and rapid induction of anesthesia. After all vital signs ceased, the animal's death was confirmed by observing the absence of respiration, heartbeat, and other vital signs for a minimum of 5 minutes. Skin sampling was then performed on the animal's carcass. The specimens were obtained from the widest area of the wound tissue with surrounding normal skin margin and were fixed in a 10% paraformaldehyde

solution for 24 h. Subsequently, they were decalcified, dehydrated with ethyl alcohol, cleared with xylene, and paraffin blocks were prepared by melting paraffin. Slides with a thickness of 7 μm were obtained from the tissue blocks using a microtome (Rotary microtome DS8402, Iran). The tissue sections were collected on glass slides, deparaffinized, and stained with H&E. Pathological changes were examined under a light microscope at ×40 magnification.

Statistical Analysis

For all data, a one-way analysis of variance (ANOVA) was used to compare between different groups. The data are presented as means ± SD, and a statistically significant difference was considered at $P < 0.05$. The statistical analyses were conducted using GraphPad Prism 8.0.0 (GraphPad Software Inc., USA).

Results

Characterizations of Nanoparticles Structure

The construction and physicochemical evaluation of TF/hIGF-1 were conducted to optimize the formulation for therapeutic application in healing diabetic wounds.

Preparation and Characterization of TF Nanoparticles

The preparation process of TF is carried out using the thin lipid film dehydration method, in which a thin lipid film is formed through the evaporation of the organic solvent. Once the thin film comes into contact with water, the sample dissolves, forming a vesicular phase that is then probe-sonicated and extruded to achieve the desired size. The results of dynamic light scattering (DLS) using the SBL algorithm for the TF obtained from 30 min of probe sonication and 11 filtration cycles showed a size of 59.03 ± 10 nm. To prevent potential damage to the protein hIGF-1, the sonication time was reduced to 10 minutes. Following these adjustments, the particle size was measured at 88.86 ± 7 nm with a uniform distribution.

Physicochemical Characterizations of TF/hIGF-1 Nanoparticles

After optimizing TF synthesis, the construction of TF/hIGF-1 nanoparticles was achieved by modifying the dehydration step. The constructed nanoparticles with a weight ratio of 1:200 (hIGF-1: lipid) were added to PBS to prepare a solution with a concentration of 50 μg/mL. The results of measuring the optimized nanoparticles including size, DPI, and zeta potential after preparation with 10 min of probe sonication and 11 filtration cycles, were as follows: a size of 57.56 ± 3 nm, PDI of 0.194, and zeta potential of −50.1 mV. Furthermore, the EE% and DL% were found to be 81.37% and 0.4%, respectively.

Transmission Electron Microscopy (TEM)

Electron microscopy investigation was conducted using TF/hIGF-1 nanoparticles negatively stained with uranyl acetate. The TEM micrographs in Figure 1 revealed that the nanoparticles exhibited dispersed spherical shapes with particle sizes below 100 nm. Although the DLS data were deemed reasonable and accurate, a slight discrepancy was observed between the results of DLS and TEM measurements. This difference can be attributed to the staining and dewatering process required for TEM samples, as well as the approximate nature of DLS in size measurement.

Short-Term Stability of Released hIGF-1

The stability of hIGF-1 after its release from TF/hIGF-1 was assessed over a 48-hour period using SDS-PAGE analysis with silver staining. A protein ladder was included in the analysis to verify the molecular mass. The electrophoretic profile revealed that all samples displayed high intensity with a distinct band migrating at an estimated molecular weight of ~8 kDa, corresponding precisely to the predicted mass of monomeric hIGF-1 (Figure 2A). Monitoring the stability profile over the 48-hour duration showed that the structural integrity of the target protein was effectively maintained. The band intensity of monomeric hIGF-1 gradually increased over the

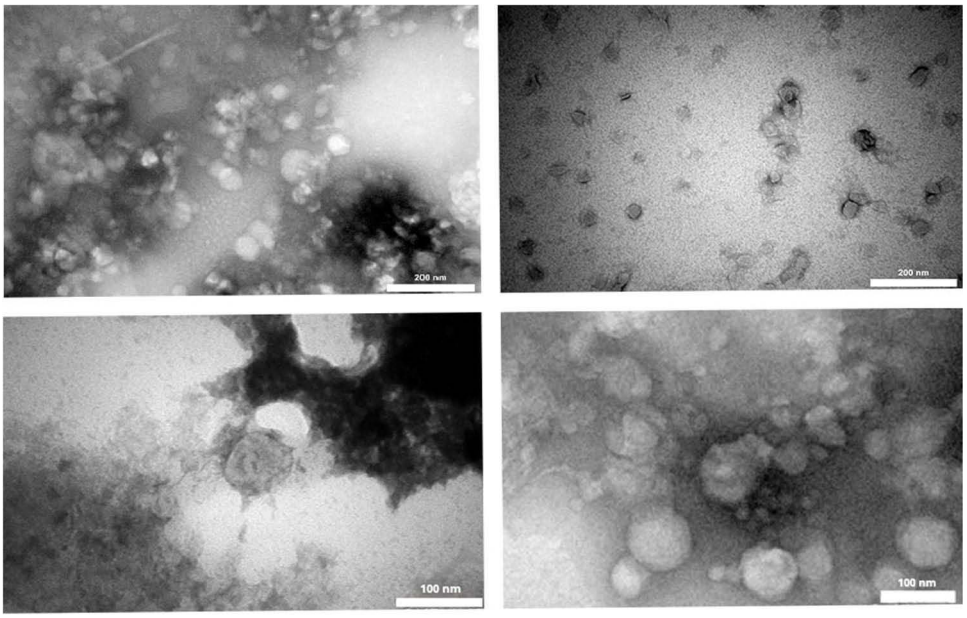

Figure 1 TEM images of the optimized TF/hIGF-1 formulation. The images display nanoparticles with dispersed spherical shapes and particle sizes below 100 nm. The scale bars represent 100 and 200 nm.

monitored time points, indicating continuous release from the nanoparticles into the physiological buffer (PBS). Importantly, no new lower molecular weight species were detected throughout the entire period, ruling out proteolytic cleavage or chemical degradation. These results demonstrate that the released hIGF-1 remains stable in the PBS environment, predominantly existing as a monomeric and homogeneous form for at least 48 hours post-release.

Diffusion Study and in vitro Release Kinetics Evaluation of hIGF-1

The in vitro release behavior of hIGF-1 from the TF/hIGF-1 was investigated through dialysis. The results of hIGF-1 release were analyzed over time using a standard release plot (Figure 2B). The results indicated that the release of hIGF-1 from the TF was significantly more controllable compared to the hIGF-1 solution. Particularly in the initial hours, only 36% of the hIGF-1 diffused from the nanoparticles, and half of the protein released from this system occurred within the first 10 h. The encapsulation of hIGF-1 in TF not only enhances drug stability but also improves its controlled delivery, as demonstrated in previous studies.[48] The kinetic profile of hIGF-1 release from the TF was evaluated using various release models to determine their equation coefficients and correlation coefficients (Table 1). The model with the highest R^2 value was considered the optimal model. Based on the analysis of the results, the Korsmeyer-Peppas model ($R^2 = 0.9582$) was identified as the best-fitted model for hIGF-1 release. This model elucidates the process of water infiltration into the matrix, swelling, and dissolution of the matrix. Furthermore, the Hixson-Crowell model, which explains release via surface dissolution ($R^2 = 0.9523$), also demonstrated a good fit.

In vitro Evaluation of Wound Healing

Cell Viability Assay

The viability and proliferation of NIH-3T3 fibroblast cells were assessed following treatment with the designed nanoparticles. The MTS assay results indicated a mitogenic effect of hIGF-1 within the first 24 h (Figure 3A). Groups treated with TF/hIGF-1 and free hIGF-1 exhibited significant cell proliferation compared to the control and TF groups. Unloaded TF did not significantly impact cell growth and proliferation. By 48 h, most therapeutic concentrations showed no significant effect on the biological activity of the growth factor due to the nanoencapsulation process (Figure 3B).

https://doi.org/10.2147/IJN.S564241

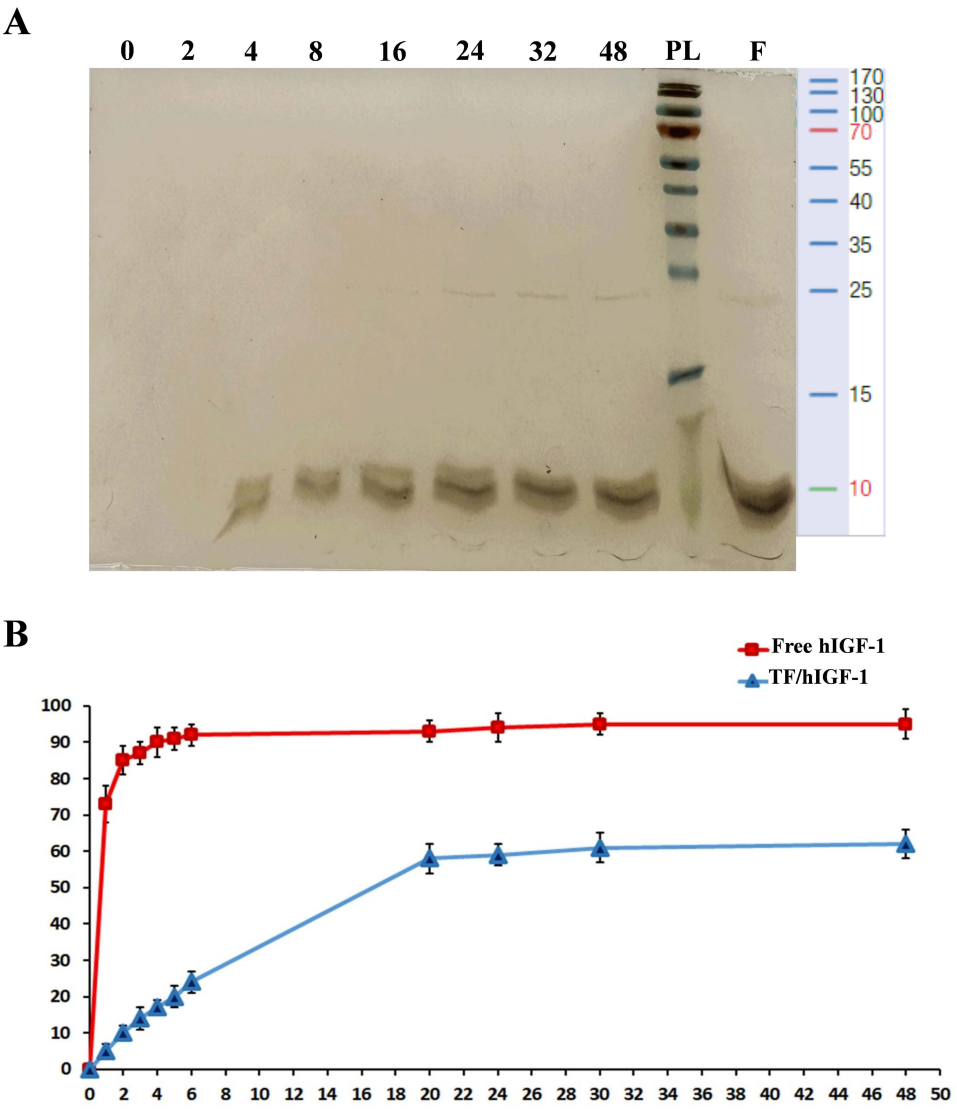

Figure 2 In vitro stability and release kinetics of hIGF-1 in TF/hIGF-1 nanoparticles. (**A**) The short-term stability of encapsulated hIGF-1 after release from TF nanoparticles was assessed using 15% SDS-PAGE analysis at various time points ranging from 0 to 48 h. (**B**) The percentage curve shows the release profile of hIGF-1 from both hIGF-1 solution and TF/hIGF-1 nanoparticles at different time points up to 48 h. PL, Protein ladder (PageRuler Prestained Protein Ladder (10–170 kDa, Thermo Fisher Scientific, USA); F, Free hIGF-1.

However, some variations were observed 72 h post-treatment (Figure 3C). Prolonged encapsulation of hIGF-1 in TF enhanced the protein's mitogenic potential compared to free hIGF-1. These findings suggest that nanoencapsulation could enhance the stability of the growth factor over 72 h, enabling the sustained delivery of hIGF-1. This, in turn, allows for continuous binding of hIGF-1 to its cell surface receptor, leading to ongoing activation of the hIGF-1 signaling pathway (Figure 3D).

Cell Migration Assay

After determining the optimal dose of TF/hIGF-1 and hIGF-1 on the NIH-3T3 cell line, the ability of hIGF-1 to promote cell migration and wound healing was evaluated using a scratch test. The results showed that the addition of 25 ng/mL hIGF-1 and 12.5 ng/mL hIGF-1 encapsulated in TF to a serum-free medium of NIH-3T3 cells significantly enhanced the cell migration after 24 h. As shown in Figure 4, cell monolayer gap was completely closed in the presence of TF/hIGF-1 containing 12.5 ng/mL of the active ingredient after 144 h compared to the control groups.

Table 1 Mathematical Modeling Illustrating the Kinetics of hIGF-1 Release from TF

Release Profile	Linear Equation	R^2	K
Zero order	$Q_T = 0.9381T + 16.0880$	0.7443	0.9381
First order	$Ln(1-Q_T) = 0.0403T + 2.7645$	0.5841	0.0403
Hixson-Crowell	$(1-Q_T)^{1/3} = -0.0352T - 1.8271$	0.9523	0.0352
Higuchi	$Q_T = 0.0582T^{1/2} + 1.3463$	0.9155	1.3463
Korsmeyer-Peppas	$Ln(Q_T) = 0.5991Ln(t) + 1.9642$	0.9582	0.0500

Abbreviations: R^2, Regression coefficient; K, Release constant.

In vivo Evaluation of Wound Healing

In vivo Studies of hIGF-1 Loaded into TF Hydrogel

We conducted a study to evaluate the efficacy of TF/hIGF-1-CMC hydrogel in promoting wound healing in diabetic rat models compared to control groups. Diabetes was induced in rats initially using STZ, and rats with blood glucose levels reaching 250 mg/dL after two days were considered diabetic. Full-thickness wounds with 8 mm diameters were then generated in the paravertebral dorsal skin of each rat. Wound healing assessments were carried out with various treatments, and results were recorded after the first wound had healed on the 12th day post-wound generation. Wound photographs were taken throughout the treatment period. As depicted in Figures 5 and 6 there was a significant difference in the wound area among the groups on day 12. The wound area treated with TF/hIGF-1 hydrogel decreased significantly compared to all other groups without hIGF-1. The wound closure in the experimental groups (hIGF-1 and TF/hIGF-1) was significantly faster than in the untreated and CMC hydrogel control groups. Besides, the wound area in the hIGF-1

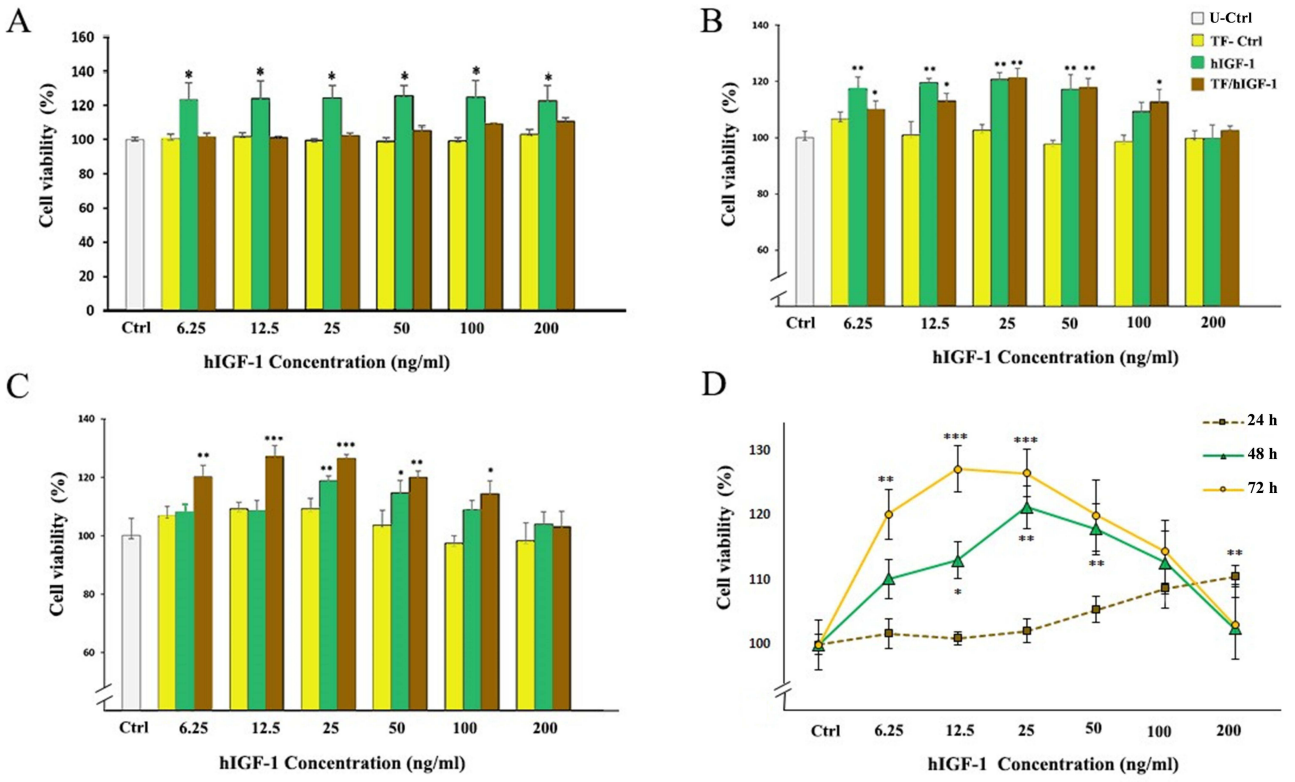

Figure 3 The survival of NIH-3T3 fibroblast cells after treatment with designed nanoparticles. The cells were cultured in DMEM medium without FBS. The graph depicts the percentage of cell survival at various concentrations after (**A**) 24 h, (**B**) 48 h, and (**C**) 72 h. (**D**) Displays the percentage of cell survival at different concentrations after 24, 48, and 72 h. (*$P < 0.05$, **$P < 0.005$, ***$P < 0.0005$ vs the control group).
Abbreviations: U-Ctrl, Untreated cells; TF-Ctrl, Empty transfersome; TF/hIGF-1, Transfersome nanoparticle containing hIGF-1.

https://doi.org/10.2147/IJN.S564241

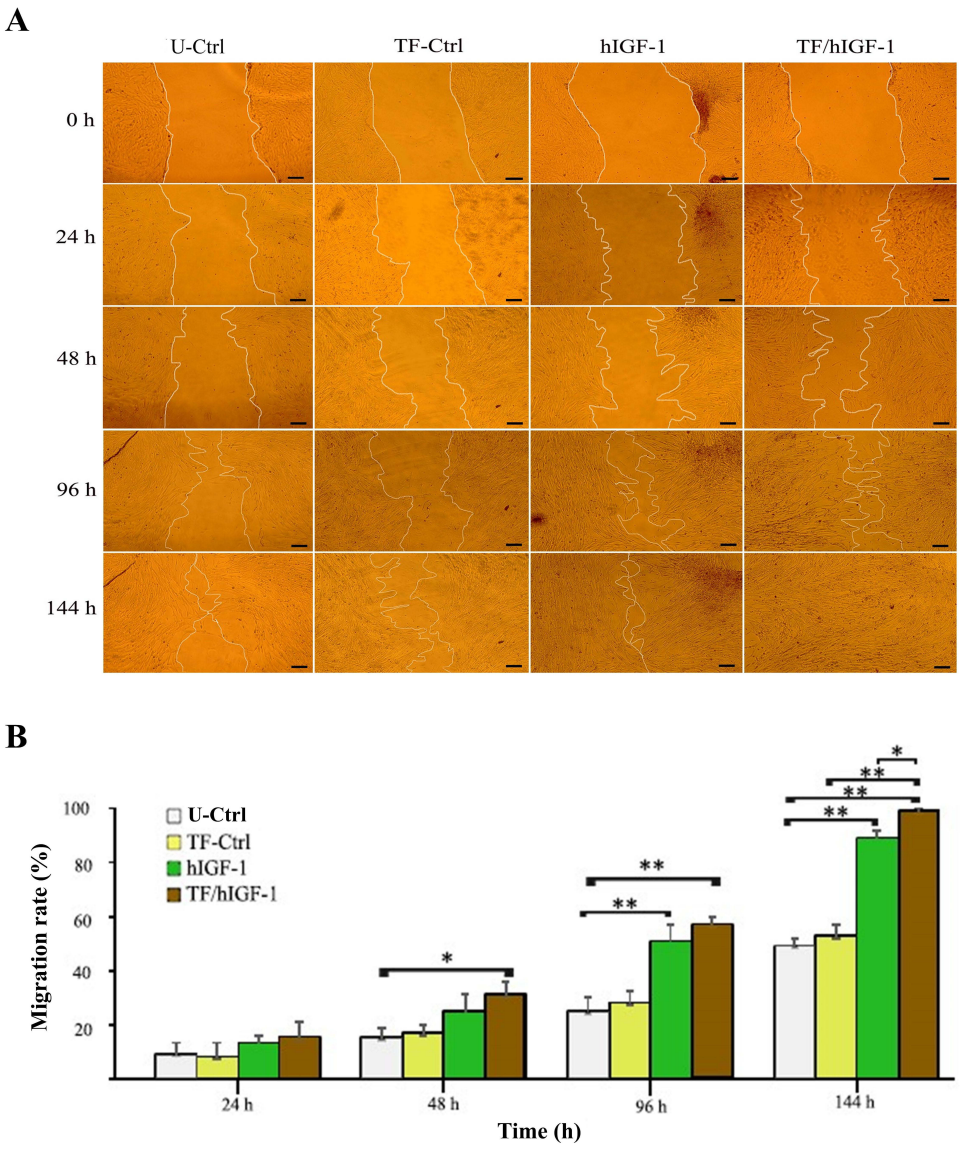

Figure 4 Effects of unloaded TF, free hIGF-1, and TF/hIGF-1 on NIH-3T3 fibroblast scratch closure compared to untreated cells. (**A**) Scratch assay conducted on NIH-3T3 fibroblast cells. The closure of the scratches, indicating cell proliferation and migration, was compared among different treatment groups (hIGF-1, TF/hIGF-1, TF) and the untreated control group at various time points up to 144 h post-scratching. The scale bar represents 100 μm. (**B**) Quantitative analysis of the migration rate among the mentioned treatment groups presented as a percentage. (*$P < 0.05$, **$P < 0.005$).
Abbreviations: U-Ctrl, Untreated cells; TF-Ctrl, Unloaded transfersome; TF/hIGF-1, Transfersome nanoparticle containing hIGF-1.

group showed a significant reduction compared to the untreated control group. Overall, the results demonstrate a significant acceleration of the wound healing process following the application of TF/hIGF-1 hydrogel compared to the other groups with almost complete healing observed by the end of the treatment period on day 12.

Histological Evaluation of Wound Healing

Both diabetic and non-diabetic animals were divided into groups: unwounded (Ctrl), untreated wounded (U-Ctrl), wounded treated with CMC hydrogel (CMC-Ctrl), wounds treated with TF containing hydrogel (TF//CMC-Ctrl), wounds treated with hIGF-1 containing hydrogel (hIGF-1/CMC), and wounds treated with TF/hIGF-1 containing hydrogel (TF/hIGF-1/CMC) groups. At the time of the first wound closure, animals were sacrificed, and skin sections were obtained from the edge of the original wounds and from the center of the recently healed wounds. Histopathological studies were conducted on skin sections to compare the effects of CMC, TF, hIGF-1, and TF/hIGF-1 in the various experimental

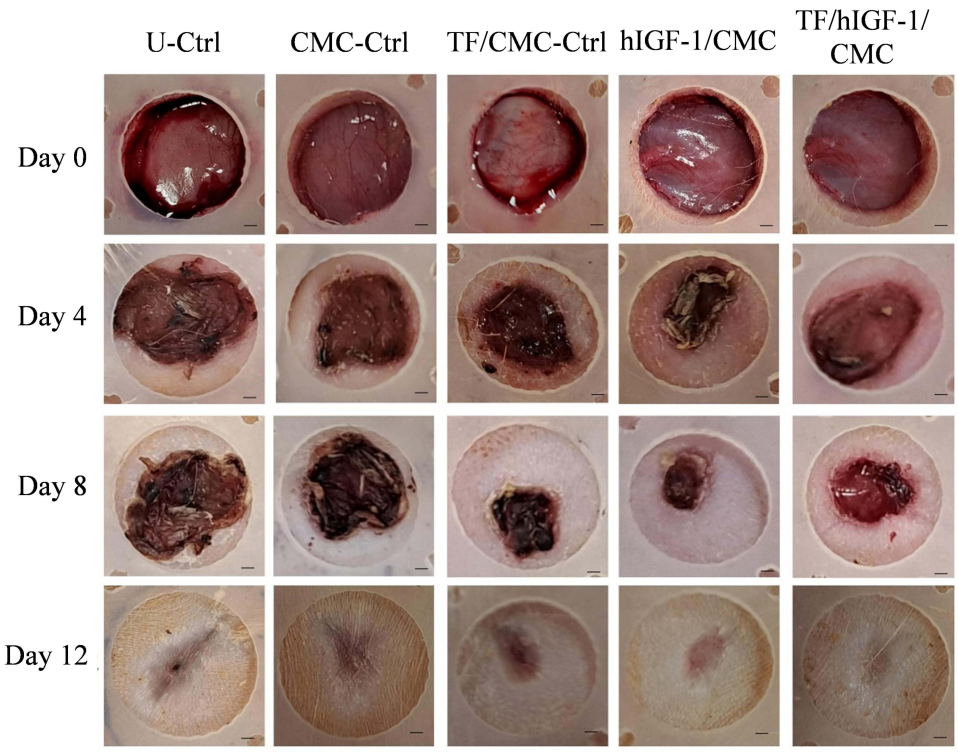

Figure 5 Time-course analysis of diabetic wound healing induced by hIGF-1. The results demonstrate wound closure in diabetic rat models following a three-stage treatment, with dressings applied once every 4 days. Scale bars in all subfigures are 0.9 mm.
Abbreviations: U-Ctrl, Untreated wound; CMC-Ctrl, Wound treated with CMC hydrogel; TF/CMC-Ctrl, Unloaded TF containing CMC hydrogel; hIGF-1/CMC, Free hIGF-1 containing CMC hydrogel; TF/hIGF-1/CMC, TF/hIGF-1 containing CMC hydrogel.

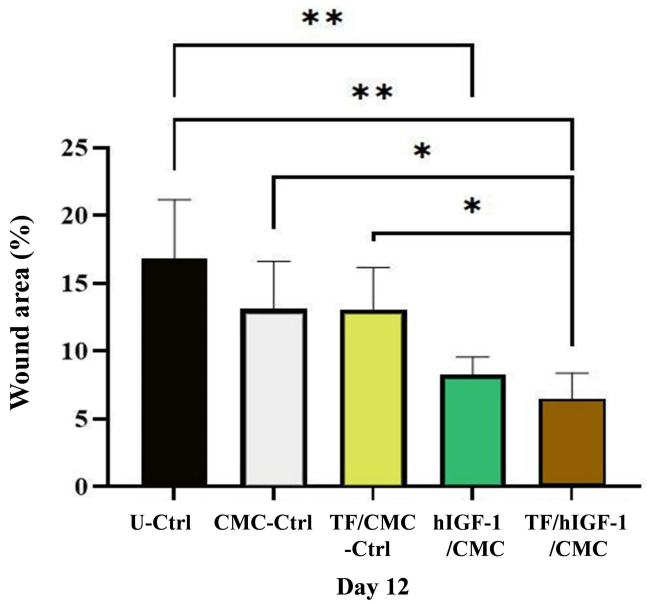

Figure 6 The statistical analysis of wound healing in five experimental groups after a 12-day treatment period. The wound area was quantified using ImageJ software. The data are presented as mean ± S.D (n = 4) (*$P < 0.05$, **$P < 0.01$ vs the control group).
Abbreviations: U-Ctrl, Untreated wound; CMC-Ctrl, Wound treated with CMC hydrogel; TF/CMC-Ctrl, Unloaded TF containing CMC hydrogel; hIGF-1/CMC, Free hIGF-1 containing CMC hydrogel; TF/hIGF-1/CMC, TF/hIGF-1 containing CMC hydrogel.

https://doi.org/10.2147/IJN.S564241

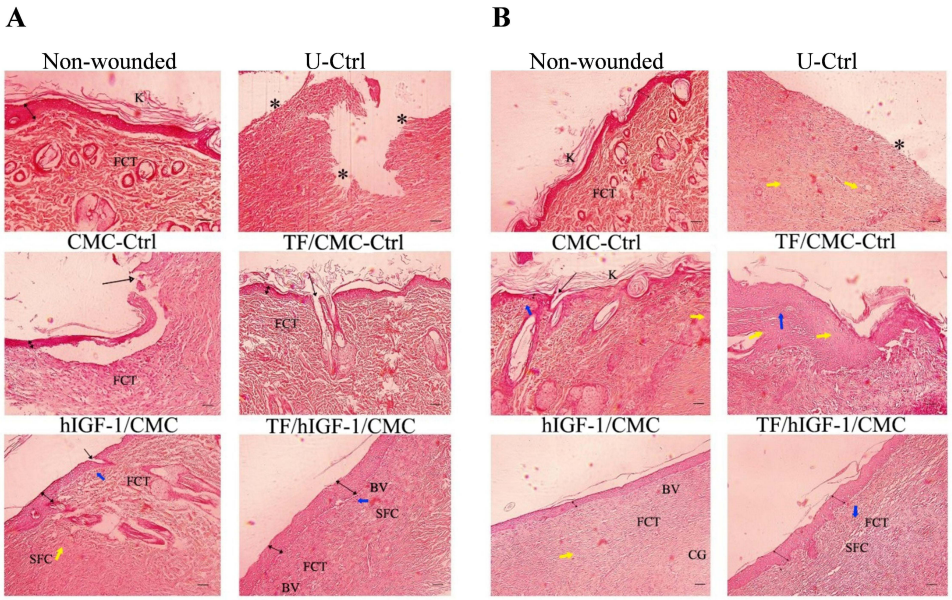

Figure 7 The histological analysis of regenerative tissue in the wound area 12 days post-treatment with hIGF-1. The representative images compare histopathological features, epithelialization, and wound healing between diabetic wounds (**A**) and non-diabetic wounds (**B**) groups after H&E staining. Black stars indicate open wounds, blue arrows indicate inflammatory cells, yellow arrows highlight fibrosis, one-sided black arrows show the superficial wound of the epidermal layer, and two-sided black arrows indicate the thickness of the epidermal layer. (The scale bar represents 50 μm (Magnification ×100).

Abbreviations: U-Ctrl, untreated wounded group; CMC-Ctrl, wounded treated with CMC hydrogel group; TF/CMC-Ctrl, wounds treated with empty TF-containing hydrogel group; hIGF-1/CMC, wounds treated with hIGF-1-containing hydrogel group; TF/hIGF-1/CMC, wounds treated with TF/hIGF-1-containing hydrogel group; SFC, Spindle fibroblast cell; FCT, Fibrous connective tissue; BV, Blood vessel; CG, Collagen; K, Keratin.

groups, including epidermal thickness, proliferation, and edema. Figure 7A and B display the histological skin sections of diabetic and non-diabetic wound areas obtained from each group, respectively. There was little difference in the appearance of the control skin between the groups. However, the epidermis of diabetic skin in the untreated group with hIGF-1 was slightly thinner than that of the treated groups (double-headed black arrows). Increased epidermal thickness and higher cell proliferation in the dermis of the TF/hIGF-1/CMC group were evident compared to the other groups. As shown in this figure, the control wound groups exhibited severe edema, disorganized microstructures, and intense infiltration of inflammatory cells. In contrast, the wound tissues in the hIGF-1/CMC and TF/hIGF-1/CMC groups showed a more well-organized tissue state compared to their controls. The distribution of inflammatory cells (blue arrows) increased in the inflammatory phase and decreased as wound healing approached, while fibrosis (yellow arrows) increased as wound healing progressed. The dilated blood vessels also increased in the acute phase of inflammation in the untreated group while they decreased as the wound entered the chronic phase or healed. The epidermis thickened in all hIGF-1 and TF/hIGF-1 groups, although it was thinner in the untreated diabetic rats. There appear to be more spindle fibroblast cells (SFCs) in the skin of non-diabetic and diabetic rats after treatment with hIGF-1 and TF/hIGF-1. Visually, these cells were observed in red granular tissues, which could be found in all of the hIGF-1 and TF/hIGF-1 treated groups. The tissue appearance in these groups suggests that the wounds were transitioning from the inflammatory phase to the healing phase during the treatment period.

Discussion

In this study, nanocarrier-based drug delivery was used to improve the healing and repair of diabetic ulcers. Dermal drug delivery by this system provides a localized and non-invasive approach to treating skin conditions, offering advantages such as continuous and prolonged drug release, increased patient satisfaction, reduced drug doses, and cost-effectiveness.[49] TF-type nanoparticles were selected as carriers due to their unique chemical properties that facilitate efficient and sustained release of therapeutic proteins into the skin. To promote the healing and repair of diabetic skin injuries, hIGF-1 was chosen and encapsulated in TF nanoparticles. This growth factor is commonly employed in the

treatment of skin wounds, fibrosis, diabetic ulcers, and inflammation. Overall, TF nanoparticles, as a drug delivery system, are expected to improve the permeability of hIGF-1 through the skin, traversing the epidermis, and finally reaching the dermis. It is also anticipated that these nanoparticles can effectively retain the drug in the dermis layer for an extended duration, thereby expediting the healing process of skin wounds, burns, and chronic diabetic ulcers. This drug delivery system has demonstrated success in delivering rivastigmine,[50] insulin,[51] and thymoquinone[52] for the treatment of Alzheimer's disease.

TFs were chosen in this study for their high deformability, enabling the continuous delivery of hIGF-1 to deeper skin layers. The composition of TFs includes Phospholipon 90 H as a phospholipid and sodium deoxycholate as a surfactant, with each ingredient playing a critical role in the carrier's properties. After designing and optimizing the experiment, the optimal TF size was determined to be 57.56 ± 3 nm with a dispersion index of 0.194. To reduce the size of the multilayer TFs, a sonicator was used to produce monolayer carriers. The resulting nanoparticles exhibited similar characteristics to previously reported TF-based nanosystems for delivering various drugs, such as insulin,[51,53,54] asenapine maleate,[55] and verapamil.[56] The zeta potential of hIGF-1 containing TF was measured at −50.1 mV. The negative charge of the carrier reduces the possibility of aggregation and mass formation over time. The encapsulation efficiency of hIGF-1 in TF was determined using the Bradford method, which showed an efficiency of 80.3% at a lipid-protein drug weight ratio of 200:1. The release of hIGF-1 from TF was assessed using the dialysis bag method, and the controlled release over 48 h was found to fit the Korsmeyer-Peppas kinetic model. In a study by Surini et al, the EF% exceeded 90% for rhEGF-loaded TF. Moreover, the particle size, PDI, and zeta potential were 128.1 ± 0.66 nm, 0.109 ± 0.004, and −43.1 ± 1.07 mV, respectively.[57] In another study where TF was used to enhance percutaneous delivery of rhEGF, a concentration of 0.025% growth factor was successfully encapsulated into the TF formulation. The mean particle size, zeta potential, and EE% were 155.57 ± 2.59 nm, −57.92 ± 4.35 mV, and 9.00 ± 0.39%, respectively.[58]

After designing and fabricating the TF/hIGF-1 nanoparticles, in vitro studies were conducted to assess their cytotoxicity using the MTS test. The viability of NIH-3T3 fibroblast cells treated with the designed nanoparticles demonstrated a mitogenic effect of hIGF-1 within the first 24 h. The groups treated with TF/hIGF-1 and free hIGF-I exhibited a significant increase in cell proliferation compared to the control groups. These findings indicate that encapsulating hIGF-1 in TF nanoparticles enhances the mitogenic potential of the growth factor over a longer period compared to free hIGF-1. Additionally, these results suggest that nanoencapsulation may improve growth factor stability over 72 h, enabling sustained delivery of hIGF-1 and continuous binding to cell surface receptors, thereby improving the activation of the hIGF-1 signaling pathway. According to studies by Dupont et al, hIGF-1R and insulin receptor are structurally similar and can activate many of the same signaling pathways, although they mediate distinct biological functions. NIH-3T3 fibroblast cells expressing the IGF-1R are stimulated by hIGF-1, which promotes the expression of IGF-1R and activates the mitogenic pathway in these cells[59] as confirmed by the results of this study. More than half of the genes regulated by hIGF-1 are associated with mitogenesis and differentiation.[60] Following the determination of the optimal doses of TF/hIGF-1 and hIGF-1 for NIH-3T3 fibroblast cells, wound healing and cell migration assays were conducted using the scratch test. The addition of 25 ng/mL hIGF-1 and 12.5 ng/mL TF/hIGF-1 to the serum-free medium significantly increased cell migration after 24 h of culture, leading to complete closure of the cell monolayer gap after 144 h in the presence of 12.5 ng/mL TF/hIGF-1 nanoparticles.

Similarly, Lin et al used a silk fibroin (SF) film as a sustained-release system for hIGF-1. The hIGF-1-loaded SF films significantly accelerated wound healing in vitro compared to wounds treated with hIGF-1 and a hIGF-1-loaded hydrocolloid dressing. Western blot analysis also showed that phosphorylation of the IGF-1R in diabetic wounds in the hIGF-1 SF film group was significantly increased compared to other experimental groups. This study demonstrated that the constant delivery of hIGF-1 from sustained-release systems promotes wound healing by continuously activating the hIGF-1 pathway, leading to improved wound re-epithelialization and tissue formation in the dermis and fibroblast cells.[2] In our study, an in vivo investigation was finally performed on male rats with induced diabetes to evaluate wound healing. The results showed a significant difference in wound area between groups on day 12. The wound area treated with TF/hIGF-1 hydrogel showed a significant acceleration of wound healing and almost complete healing on day 12 after the application of TF/hIGF-1 hydrogel compared to the other groups without hIGF-1. It is believed that the TF

nanoparticles penetrates deeper into the skin tissue and maintains the controlled release of the growth factor throughout the 12-day treatment period.

Previous studies have shown that wounds treated with hIGF-1 exhibit faster re-epithelialization by enhancing dermal cell migration and viability.[16,61] Furthermore, preliminary immunohistochemical analysis revealed a significant increase in myofibroblasts, which are key cells that appear during the proliferative phase and produce collagen and extracellular matrix to regenerate damaged tissue. This indicates that hIGF-1 actively promotes the reconstruction of the wound dermal layer by enhancing collagen synthesis.[62,63] In our study, histopathological examination also showed minimal differences in the appearance of control skin between groups. However, the diabetic epidermis of the TF/hIGF-1 and hIGF-1 untreated groups was slightly thinner than that of the treated groups (indicated by double-headed arrows). The TF/hIGF-1 group exhibited an increase in epidermal thickness and appendages in the dermis compared to the other groups, suggesting a better-organized histological state. Conversely, the control groups showed severe edema, disorganized microstructures, and intense infiltration of inflammatory cells, indicating a less organized histological appearance. Meanwhile, the thicker epidermis and more spindle-shaped fibroblasts in the hIGF-1 and TF/hIGF-1 groups, along with the thinner epidermis in the wounds of untreated diabetic rats, also confirmed the superior therapeutic effects of TF/hIGF-1. Similarly, in the study by Lin et al, they used hIGF-1 hydrocolloid treatments encapsulated in silk fibroin (SF-hIGF-1) to heal diabetic wounds over a 12-day treatment period. The closure of wounds treated with SF-hIGF-1 was faster compared to those treated with PBS or hIGF-1 alone. Furthermore, the SF-hIGF-1 treatment resulted in smoother surfaces, indicating increased angiogenesis in diabetic wounds relative to the controls.[2]

Conclusion

In this study, TF/hIGF-1 nanoparticles were synthesized and characterized with the optimal formulation. The results demonstrated that hIGF-1 was well-encapsulated in TF at an appropriate size and in an amorphous state. The application of these nanoparticles in a CMC hydrogel formulation revealed that TF facilitated the transport of hIGF-1 into the skin epithelium and significantly improved the prolonged release of hIGF-1 to the wound . Additionally, an in vivo study showed accelerated wound closure after only 12 days compared to the control group, and histopathology tests of the wounds confirmed that TF/hIGF-1 could enhance epidermal thickness and dermis regeneration indicating enhanced diabetic wound healing effects due to the controlled-release and regenerative effect of hIGF-1. These findings suggest a promising new approach for rapid and effective treatment of diabetic wounds. We believe that this approach could potentially be applied for skin regeneration in other skin disorders such as fibrosis and inflammation. It is worth noting that we did not investigate the TF/hIGF-1 mechanism of action in accelerating the repair of diabetic wounds in this study. A comprehensive understanding of this mechanism in future studies can help to improve the therapeutic effect and safety of this formulation.

Data Sharing Statement

Data will be made available on request by contacting the corresponding author.

Acknowledgments

We acknowledge the assistance of Royan Institute for Biotechnology for its services and facilities.

Funding

This work was supported by the Royan Lotus Charity Fund (NO. 140102001/296584).

Disclosure

The authors declare that there is no conflict of interest in this study.

References

1. Lin MJ, Lu MC, Chan YC, Huang YF, Chang HY. An insulin-like growth factor-1 conjugated bombyx mori silk fibroin film for diabetic wound healing: fabrication, physicochemical property characterization, and dosage optimization in vitro and in vivo. *Pharmaceutics*. 2021;13(9):1459. doi:10.3390/pharmaceutics13091459
2. Lin MJ, Lu MC, Chang HY. Sustained release of insulin-like growth factor-1 from Bombyx mori L. silk fibroin delivery for diabetic wound therapy. *Int J Mol Sci*. 2021;22(12):6267. doi:10.3390/ijms22126267
3. Bailes J, Soloviev M. Insulin-like growth factor-1 (IGF-1) and its monitoring in medical diagnostic and in sports. *Biomolecules*. 2021;11(2):217. doi:10.3390/biom11020217
4. Rosenbloom AL. Mecasermin (recombinant human insulin-like growth factor I). *Adv Ther*. 2009;26(1):40–54. doi:10.1007/s12325-008-0136-5
5. Kemp SF, Frindik JP. Emerging options in growth hormone therapy: an update. *Drug Des Devel Ther*. 2011;5:411–419. doi:10.2147/DDDT.S23140
6. Clemmons DR. Metabolic actions of insulin-like growth factor-I in normal physiology and diabetes. *Endocrinol Metab Clin North Am*. 2012;41(2):425–43,vii–viii. doi:10.1016/j.ecl.2012.04.017
7. Yakar S, Adamo ML. Insulin-like growth factor 1 physiology: lessons from mouse models. *Endocrinol Metab Clin North Am*. 2012;41(2):231–47,v. doi:10.1016/j.ecl.2012.04.008
8. Cheng S, Lv R, Xu J, Hirman AR, Du L. IGF-1-expressing placenta-derived mesenchymal stem cells promote scalding wound healing. *J Surg Res*. 2021;265:100–113. doi:10.1016/j.jss.2021.02.057
9. Lin M, Liu X, Zheng H, et al. IGF-1 enhances BMSC viability, migration, and anti-apoptosis in myocardial infarction via secreted frizzled-related protein 2 pathway. *Stem Cell Res Ther*. 2020;11(1):22. doi:10.1186/s13287-019-1544-y
10. Haase I, Evans R, Pofahl R, watt FM. Regulation of keratinocyte shape, migration and wound epithelialization by IGF-1-and EGF-dependent signalling pathways. *J Cell Sci*. 2003;116(15):3227–3238. doi:10.1242/jcs.00610
11. Seeger MA, Paller AS. The roles of growth factors in keratinocyte migration. *Adv Wound Care*. 2015;4(4):213–224. doi:10.1089/wound.2014.0540
12. Lin S, Zhang Q, Shao X, et al. IGF-1 promotes angiogenesis in endothelial cells/adipose-derived stem cells co-culture system with activation of PI3K/Akt signal pathway. *Cell Prolif*. 2017;50(6):e12390. doi:10.1111/cpr.12390
13. Berlanga-Acosta J, Schultz GS, López-Mola E, Guillen-Nieto G, García-Siverio M, Herrera-Martínez L. Glucose toxic effects on granulation tissue productive cells: the diabetics' impaired healing. *Biomed Res Int*. 2013;2013(1):256043. doi:10.1155/2013/256043
14. Capla JM, Grogan RH, Callaghan MJ, et al. Diabetes impairs endothelial progenitor cell-mediated blood vessel formation in response to hypoxia. *Plast Reconstr Surg*. 2007;119(1):59–70. doi:10.1097/01.prs.0000244830.16906.3f
15. Velander P, Theopold C, Hirsch T, et al. Impaired wound healing in an acute diabetic pig model and the effects of local hyperglycemia. *Wound Repair Regen*. 2008;16(2):288–293. doi:10.1111/j.1524-475X.2008.00367.x
16. Garoufalia Z, Papadopetraki A, Karatza E, et al. Insulin-like growth factor-I and wound healing, a potential answer to non-healing wounds: a systematic review of the literature and future perspectives. *Biomed Rep*. 2021;15(2):1–5. doi:10.3892/br.2021.1442
17. Brown DL, Kane CD, Chernausek SD, Greenhalgh DG. Differential expression and localization of insulin-like growth factors I and II in cutaneous wounds of diabetic and nondiabetic mice. *Am J Pathol*. 1997;151(3):715.
18. Rask-Madsen C, King GL. Mechanisms of disease: endothelial dysfunction in insulin resistance and diabetes. *Nat Clin Pract Endocrinol Metab*. 2007;3(1):46–56. doi:10.1038/ncpendmet0366
19. Berlanga-Acosta J, Camacho-Rodríguez H, Mendoza-Marí Y, et al. Epidermal growth factor in healing diabetic foot ulcers: from gene expression to tissue healing and systemic biomarker circulation. *MEDICC Rev*. 2022;22:24–31.
20. Tavakkol A, Elder JT, Griffiths CE, et al. Expression of growth hormone receptor, insulin-like growth factor 1 (IGF-1) and IGF-1 receptor mRNA and proteins in human skin. *J Invest Dermatol*. 1992;99(3):343–349. doi:10.1111/1523-1747.ep12616668
21. Sadagurski M, Yakar S, Weingarten G, et al. Insulin-like growth factor 1 receptor signaling regulates skin development and inhibits skin keratinocyte differentiation. *Mol Cell Biol*. 2006;26(7):2675–2687. doi:10.1128/MCB.26.7.2675-2687.2006
22. Weger N, Schlake T. Igf-I signalling controls the hair growth cycle and the differentiation of hair shafts. *J Invest Dermatol*. 2005;125(5):873–882. doi:10.1111/j.0022-202X.2005.23946.x
23. Pierre E, Perez-Polo JR, Mitchell AT, Matin S, Foyt HL, Herndon DN. Insulin-like growth factor-I liposomal gene transfer and systemic growth hormone stimulate wound healing. *J Burn Care Rehabil*. 1997;18(4):287–291. doi:10.1097/00004630-199707000-00002
24. Gillery P, Leperre A, Maquart FX, Borel JP. Insulin-like growth factor-I (IGF-I) stimulates protein synthesis and collagen gene expression in monolayer and lattice cultures of fibroblasts. *J Cell Physiol*. 1992;152(2):389–396. doi:10.1002/jcp.1041520221
25. Hirsch T, Spielmann M, Velander P, et al. Insulin-like growth factor-1 gene therapy and cell transplantation in diabetic wounds. *J Gene Med*. 2008;10(11):1247–1252. doi:10.1002/jgm.1251
26. Aboutalebi F, Lachinani L, Khazaei Y, et al. An efficient method for bacterial production and activity assessment of recombinant human insulin like growth factor 1. *Mol Biol Rep*. 2018;45:1957–1966. doi:10.1007/s11033-018-4348-8
27. Zhang X, Hu F, Li J, et al. IGF-1 inhibits inflammation and accelerates angiogenesis via Ras/PI3K/IKK/NF-κB signaling pathways to promote wound healing. *Eur J Pharm Sci*. 2024;200:106847. doi:10.1016/j.ejps.2024.106847
28. Kushwaha SK, Keshari RK, Rai A. Advances in nasal trans-mucosal drug delivery. *J Appl Pharm Sci*. 2011;01(07):21–28.
29. Di Cola G, Cool MH, Accili D. Hypoglycemic effect of insulin-like growth factor-1 in mice lacking insulin receptors. *J Clin Invest*. 1997;99(10):2538–2544. doi:10.1172/JCI119438
30. Bos JD, Meinardi MM. The 500 dalton rule for the skin penetration of chemical compounds and drugs. *Exp Dermatol*. 2000;9(3):165–169. doi:10.1034/j.1600-0625.2000.009003165.x
31. Yu DG, He W, He C, Liu H, Yang H. Versatility of electrospun Janus wound dressings. *Nanomedicine*. 2025;20(3):271–278. doi:10.1080/17435889.2024.2446139
32. Hu Y, Zhang F, Zhou J, et al. Electrospun tri-layer core-sheath nanofibrous coating for sequential treatment of postoperative complications in orthopedic implants. *Small*. 2025;21(42):e05523. doi:10.1002/smll.202505523
33. Ganji F, Vasheghani-Farahani E. Hydrogels in controlled drug delivery systems. *Iran Polym J*. 2009;18(1):63–88.
34. Levin G, Gershonowitz A, Sacks H, et al. Transdermal delivery of human growth hormone through RF-microchannels. *Pharm Res*. 2005;22:550–555. doi:10.1007/s11095-005-2498-6

35. Jacob L, Anoop K. A review on surfactants as edge activators in ultradeformable vesicles for enhanced skin delivery. *Int J Pharm Biol Sci*. 2013;4 (3):337–344.
36. Opatha SAT, Titapiwatanakun V, Chutoprapat R. Transfersomes: a promising nanoencapsulation technique for transdermal drug delivery. *Pharmaceutics*. 2020;12(9):855. doi:10.3390/pharmaceutics12090855
37. Bnyan R, Khan I, Ehtezazi T, et al. Surfactant effects on lipid-based vesicles properties. *J Pharm Sci*. 2018;107(5):1237–1246. doi:10.1016/j.xphs.2018.01.005
38. Gupta A, Aggarwal G, Singla S, Arora R. Transfersomes: a novel vesicular carrier for enhanced transdermal delivery of sertraline: development, characterization, and performance evaluation. *Sci Pharm*. 2012;80(4):1061. doi:10.3797/scipharm.1208-02
39. Su Z, Wu S, Zhang H, Feng Y. Development and validation of an improved Bradford method for determination of insulin from chitosan nanoparticulate systems. *Pharm Biol*. 2010;48(9):966–973. doi:10.3109/13880200903325615
40. Chevallet M, Luche S, Rabilloud T. Silver staining of proteins in polyacrylamide gels. *Nat Protoc*. 2006;1(4):1852–1858. doi:10.1038/nprot.2006.288
41. Che Nan N, Zainuddin N, Ahmad M. Preparation and swelling study of CMC hydrogel as potential superabsorbent. *Pertanika J Sci Technol*. 2019;27(1):489–498.
42. El-Samad LM, Hassan MA, Basha AA, et al. Carboxymethyl cellulose/sericin-based hydrogels with intrinsic antibacterial, antioxidant, and anti-inflammatory properties promote re-epithelization of diabetic wounds in rats. *Int J Pharm*. 2022;629:122328. doi:10.1016/j.ijpharm.2022.122328
43. Ghasemi A, Jeddi S. Streptozotocin as a tool for induction of rat models of diabetes: a practical guide. *EXCLI J*. 2023;22:274. doi:10.17179/excli2022-5720
44. Ahmadi-Noorbakhsh S, Mirabzadeh Ardakani E, Sadighi J, et al. Guideline for the care and use of laboratory animals in Iran. *Lab Animal*. 2021;50 (11):303–305. doi:10.1038/s41684-021-00871-3
45. Zhou J, Ni M, Liu X, Ren Z, Zheng Z. Curcumol promotes vascular endothelial growth factor (VEGF)-mediated diabetic wound healing in streptozotocin-induced hyperglycemic rats. *Med Sci Monit*. 2017;23:555. doi:10.12659/MSM.902859
46. Kamar SS, Abdel-Kader DH, Rashed LA. Beneficial effect of curcumin nanoparticles-hydrogel on excisional skin wound healing in type-I diabetic rat: histological and immunohistochemical studies. *Ann Anat*. 2019;222:94–102. doi:10.1016/j.aanat.2018.11.005
47. Leary S, Underwood W, Anthony R, et al. *AVMA Guidelines for the Euthanasia of Animals*. 2020 ed. Schaumburg, IL, USA: American Veterinary Medical Association; 2020.
48. Patel R, Singh S, Singh S, Sheth N, Gendle R. Development and characterization of curcumin loaded transfersome for transdermal delivery. *J Pharm Sci Res*. 2009;1(4):71.
49. Gowda BH, Mohanto S, Singh A, et al. Nanoparticle-based therapeutic approaches for wound healing: a review of the state-of-the-art. *Mater Today Chem*. 2023;27:101319.
50. Fazil M, Md S, Haque S, et al. Development and evaluation of rivastigmine loaded chitosan nanoparticles for brain targeting. *Eur J Pharm Sci*. 2012;47(1):6–15. doi:10.1016/j.ejps.2012.04.013
51. Nojoki F, Ebrahimi-Hosseinzadeh B, Hatamian-Zarmi A, Khodagholi F, Khezri K. Design and development of chitosan-insulin-transfersomes (Transfersulin) as effective intranasal nanovesicles for the treatment of Alzheimer's disease: in vitro, in vivo, and ex vivo evaluations. *Biomed Pharmacother*. 2022;153:113450. doi:10.1016/j.biopha.2022.113450
52. Alam S, Khan ZI, Mustafa G, et al. Development and evaluation of thymoquinone-encapsulated chitosan nanoparticles for nose-to-brain targeting: a pharmacoscintigraphic study. *Int J Nanomed*;2012. 5705–5718. doi:10.2147/IJN.S35329
53. Marwah H, Garg T, Rath G, Goyal AK. Development of transferosomal gel for trans-dermal delivery of insulin using iodine complex. *Drug Deliv*. 2016;23(5):1636–1644. doi:10.3109/10717544.2016.1155243
54. Cevc G, Gebauer D, Stieber J, Schaetzlein A, Blume G. Transfersomes, have an extremely low pore penetration resistance and transport therapeutic amounts of insulin across the intact mammalian skin. *Biochim Biophys Acta*. 1998;1368:201–215. doi:10.1016/S0005-2736(97)00177-6
55. Shreya A, Managuli RS, Menon J, et al. Nano-transfersomal formulations for transdermal delivery of asenapine maleate: in vitro and in vivo performance evaluations. *J Liposome Res*. 2016;26(3):221–232. doi:10.3109/08982104.2015.1098659
56. Mouez MA, Nasr M, Abdel-Mottaleb M, Geneidi AS, Mansour S. Composite chitosan-transfersomal vesicles for improved transnasal permeation and bioavailability of verapamil. *Int J Biol Macromol*. 2016;93:591–599. doi:10.1016/j.ijbiomac.2016.09.027
57. Surini S, Leonyza A, Suh CW. Formulation and in vitro penetration study of recombinant human epidermal growth factor-loaded transfersomal emulgel. *Adv Pharm Bull*. 2020;10(4):586. doi:10.34172/apb.2020.070
58. Jeon SO, Hwang HJ, Oh DH, et al. Enhanced percutaneous delivery of recombinant human epidermal growth factor employing nano-liposome system. *J Microencapsul*. 2012;29(3):234–241. doi:10.3109/02652048.2011.646327
59. Dupont J, Fernandez AM, Glackin CA, Helman L, LeRoith D. Insulin-like growth factor 1 (IGF-1)-induced twist expression is involved in the anti-apoptotic effects of the IGF-1 receptor. *J Biol Chem*. 2001;276(28):26699–26707. doi:10.1074/jbc.M102664200
60. Hofmann C, Goldfine I, Whittaker J. The metabolic and mitogenic effects of both insulin and insulin-like growth factor are enhanced by transfection of insulin receptors into NIH3T3 fibroblasts. *J Biol Chem*. 1989;264(15):8606–8611. doi:10.1016/S0021-9258(18)81835-X
61. Achar RA, Silva TC, Achar E, Martines RB, Machado JL. Use of insulin-like growth factor in the healing of open wounds in diabetic and non-diabetic rats. *Acta Cir Bras*. 2014;29(02):125–131. doi:10.1590/S0102-86502014000200009
62. Darby IA, Laverdet B, Bonté F, Desmoulière A. Fibroblasts and myofibroblasts in wound healing. *Clin Cosmet Invest Dermatol*. 2014;7:301–311. doi:10.2147/CCID.S50046
63. Xia Y, Chen J, Ding J, Zhang J, Chen H. IGF1- and BM-MSC-incorporating collagen-chitosan scaffolds promote wound healing and hair follicle regeneration. *Am J Transl Res*. 2020;12(10):6264–6276.